Available online at www.sciencedirect.com
ScienceDirect
Scripta Materialia 56 (2007) 313–316
Scripta MATERIALIA
www.actamat-journals.com

Contribution to size effect of yield strength from the stochastics of dislocation source lengths in finite samples

Triplicane A. Parthasarathy,[a,*] Satish I. Rao,[a] Dennis M. Dimiduk,[b] Michael D. Uchic[b] and Dallas R. Trinkle[b]

[a] *UES, Inc., 4401 Dayton-Xenia Road, Dayton, OH 45432, USA*
[b] *Air Force Research Laboratory, Materials and Manufacturing Directorate, AFRL/MLLM, Wright-Patterson AFB, OH 45433-7817, USA*

Received 21 July 2006; revised 8 September 2006; accepted 9 September 2006
Available online 30 October 2006

Recent works show that the yield strength of metals increases steeply with decreasing sample size. In this work, it is shown that this sample size effect can be rationalized almost completely by considering the stochastics of dislocation source lengths in samples of finite size. The statistical first and second moments of the effective source length are derived as a function of sample size. The sample strength predicted from this effective length compares well with data.
© 2006 Acta Materialia Inc. Published by Elsevier Ltd. All rights reserved.

Keywords: Size; Yield; Stochastics; Dislocation; Source

Recent works, using samples machined from nickel and gold, have shown that critical resolved shear stress for single crystal samples in compression increases significantly when the diameter of the samples are below about 10 μm [1–4]. In these cases the imposed strains are nominally uniform, and thus this phenomenon is different from that in which strengthening from gradients of imposed strain was reported [5,6]. This phenomenon also differs from earlier findings on metal whiskers of small diameter, which concluded that the phenomenon was due to the absence of dislocations and high surface quality, which prevents easy nucleation [7–9]. The microcrystals of recent works are different in that they have high strengths despite possessing relatively high dislocation densities [2]. These results have challenged the known mechanistic models of yielding in metals.

There have been several recent attempts to rationalize these findings. Sevillano et al. [10] drew an analogy with invasion percolation, as in fluid flow through a porous medium, while Greer et al. [3] suggested that the effect arises from 'starvation' of mobile dislocations as they exit the finite sized sample. Deshpande et al. [11] verified the suggestion of Greer et al., and their simulations supported the starvation model [3,11]. Balint et al. [12] suggested that starvation arises from the lack of internal nucleation events in small samples. Benzerga and Shaver conducted simulations using constitutive rules and suggested that the strengthening effect arises from internal stresses and from the dislocation source length variation with sample dimensions [13]. Volkert and Lilleodeen suggested the possibility of the loss of dislocations from the attractive effect of free surface image stresses [4].

In this work, the concept of starvation of dislocation is examined quantitatively.

In bulk solids, where availability of dislocations is not an issue, the critical resolved shear stress is largely determined by the stress required to initiate and maintain dislocation multiplication in the presence of a dislocation forest. The microplastic flow is known to initiate by multiplication of dislocations from the weakest source, typically a double-pinned Frank–Read source. The dislocations thus generated glide, interacting with other dislocations in the solid and generating further dislocations by cross-slip processes. The critical resolved shear stress (CRSS) is the stress required for the first percolation of a dislocation across the sample, often bypassing obstacles by cross-slip or by leaving loops around them [10]. In finite samples of limited dimensions, these two processes are affected in the following way.

First, the double-ended sources upon operation interact with the free surfaces and result in truncated single arms of dislocations, as shown schematically in Figure 1a. Analysis of the interaction of such a source with

* Corresponding author. E-mail: triplicane.parthasarathy@wpafb.af.mil

1359-6462/$ - see front matter © 2006 Acta Materialia Inc. Published by Elsevier Ltd. All rights reserved.
doi:10.1016/j.scriptamat.2006.09.016

the cylindrical free surface is complex, but it is a good approximation to assume that image stresses from the free surface always tend to rotate the dislocation line until it is normal to the surface [14]. Thus the stress required to move these truncated arms depends on the shortest distance from the pin to the free surface. This effect has been observed recently in large-scale three-dimensional dislocation simulations [15]. This effect is dominant when the sample size is of the same order as the spacing between internal obstacles (e.g. forest dislocations). Second, the distance a dislocation moves is limited to the width of the sample, lowering the possibility of cross-slip multiplication. Both effects contribute to starvation, leaving fewer mobile dislocations than are necessary to accommodate the externally imposed strain rate.

In finite samples, where the sample dimensions are of the same order of magnitude as the source lengths, all sources end up as being single-ended due to interaction with the free surface, as in Figure 1b. Accordingly, the model assumes a random distribution of pins in the sample, with each pin having a dislocation arm starting from it and ending at the surface. For a given pin, the length of interest is the shortest distance from the pin to the surface. Further, for a solid with several such sources, the arm that has the longest length determines the critical stress to initiate plastic strain. Thus the model calculates the longest of the arms each of which has a length that is the shortest from a pin to the surface. This will give the lower bound on the athermal CRSS in the micro-strain regime.

Consider a cylindrical specimen of radius R, with the primary slip plane oriented at an angle β from the tensile axis. The glide plane in this case is an ellipse with major axis $b = R/\cos(\beta)$ and minor axis R. For a random distribution of pins, the probability, $p(r)\mathrm{d}r$, of finding a pin within an elliptical annulus of infinitesimal width, $\mathrm{d}r$, at a distance r from the free surface is given by

$$p(r)\mathrm{d}r = \frac{\pi[(R-r)+(b-r)]}{\pi Rb}\mathrm{d}r; \quad b = R/\cos(\beta) \tag{1}$$

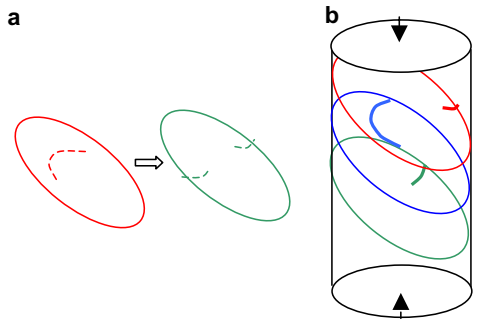

Figure 1. (a) A schematic sketch of how double-pinned Frank–Read sources quickly become single-ended sources in samples of finite dimensions. (b) Schematic sketch of single-ended sources in a finite cylindrical sample in critical configuration, which occur where the distance from the pin to the free surface is the shortest. The longest arm among the available sources (blue in this case) determines the critical resolved shear stress. Thus the statistics of pins within a sample of finite size determines the yield strength of the sample. (For interpretation of the references in colour in this figure caption, the reader is referred to the web version of this article.)

For the case of n pins located randomly, the probability for the maximum distance from the free surface to be $\lambda_{\max}$, is given by

$$p(\lambda_{\max})\mathrm{d}\lambda_{\max} = \left[1 - \frac{\pi(R-\lambda_{\max})(b-\lambda_{\max})}{\pi Rb}\right]^{n-1} \times \left(\frac{\pi[(R-\lambda_{\max})+(b-\lambda_{\max})]}{\pi Rb}\right) n\mathrm{d}\lambda_{\max} \tag{2}$$

The above equation gives the probability that a given sample with n pins has $\lambda_{\max}$ as the effective source length. The first moment of this distribution will give the mean effective source length of multiple (statistically sufficient number of) samples. The second moment will give the scatter. Thus the first and second moments of this distribution give the mean and standard deviation of the effective source length, $\lambda_{\max}$, as

$$\begin{aligned}\bar{\lambda}_{\max} &= \int_0^R \lambda_{\max} p(\lambda_{\max})\mathrm{d}\lambda_{\max} \\ &= \int_0^R \left[1 - \frac{\pi(R-\lambda_{\max})(b-\lambda_{\max})}{\pi Rb}\right]^{n-1} \\ &\quad \times \left(\frac{\pi[(R-\lambda_{\max})+(b-\lambda_{\max})]}{\pi Rb}\right) n\lambda_{\max}\mathrm{d}\lambda_{\max}\end{aligned} \tag{3}$$

$$\begin{aligned}\sigma_{\lambda_{\max}} &= \left[\int_0^R \lambda_{\max}^2 p(\lambda_{\max})\mathrm{d}\lambda_{\max} - \bar{\lambda}_{\max}^2\right]^{1/2} \\ &= \left[\int_0^R \left[1 - \frac{\pi(R-\lambda_{\max})(b-\lambda_{\max})}{\pi Rb}\right]^{n-1} \right. \\ &\quad \left. \times \left(\frac{\pi[(R-\lambda_{\max})+(b-\lambda_{\max})]}{\pi Rb}\right) n\lambda_{\max}^2\mathrm{d}\lambda_{\max} - \bar{\lambda}_{\max}^2\right]^{1/2}\end{aligned} \tag{4}$$

Both can be reduced to analytical expressions involving the generalized hypergeometric functions.

The stress required to operate a source with one end pinned and the other at the free surface of a cylinder is taken to have the same form as that for a Frank–Read source, although the appropriate geometrical factor is uncertain. This stress is the excess required over the friction stress and the stress from the dislocation forest (which results in a back stress) given by the Taylor equation, since multiple iterations of the source operation will be required for macroscopic strains of the order of 0.2%. The model neglects the effect of sample size on the possible truncation of the Taylor potential. Thus the critical resolved shear strength of a cylindrical sample, R, of height h, with the primary slip plane oriented at an angle, β, to the load axis, is then given by

$$\mathrm{CRSS} = \frac{\alpha Gb}{\bar{\lambda}_{\max}} + \tau_0 + 0.5Gb\sqrt{\rho_{\mathrm{tot}}} \tag{5}$$

where α is a geometrical constant, G the shear modulus, b the Burgers vector, τ_0 the friction stress and ρ_{tot} the total dislocation density. The mean value of source length, $\bar{\lambda}$, is given by Eq. (3), where the number of pins, n, is related to sample dimensions and initial dislocation density in the sample, as given by

$$n = \text{Integer}\left[\rho_{\text{mob}}\frac{\pi R^2 h}{L_{\text{seg}}}\right]; \quad \rho_{\text{mob}} = \frac{\rho_{\text{tot}}}{s} \tag{6}$$

where ρ_{tot}, ρ_{mob} are the total and mobile dislocation density, h is the specimen height, L_{seg} the average length of dislocation segments in the sample and s the number of slip systems, which is 12 for face-centered cubic crystals. Eq. (4) for ρ_{mob} assumes that one of the slip systems is favorably oriented and thus determines the critical resolved shear stress. The average segment length, L_{seg}, of the dislocations was taken to be R, the sample radius. To distinguish from metal whiskers which are dislocation free ($<10^{10}/\text{m}^2$), in this model for microcrystals which are known to have a dislocation density of the order of $10^{12}/\text{m}^2$, the lower bound for n is taken to be unity.

Some of the experimental data include microcrystals which are so small ($\leqslant 0.5$ μm) as to be free of dislocations, even with an average density of $10^{12}/\text{m}^2$. In these crystals, CRSS may be determined by the stress required to nucleate a dislocation from the free surface. This will still be different from whiskers, since the surfaces of microcrystals are prepared differently and the microcrystals are tested under compression, with one end still fixed to a bulk sample. Thus nucleation could occur much more easily than in whiskers. However, nucleation of the partial $1/6\langle 1\,1\,2\rangle$ is more likely from energetic considerations, and has been observed in atomistic simulations [16]. The glide of these dislocations will be limited by the trailing stacking fault in their wake [16]. Based on these arguments, the current model includes a maximum bound for the critical resolved shear stress for very small microcrystals. The stress required to nucleate from a rough surface is beyond the scope of this work, but, assuming that the CRSS is not nucleation limited, the stress to move this partial dislocation is taken to be the upper bound on CRSS. This stress will depend on the stacking fault energy, γ, and is given by

$$\text{CRSS}(\max) = (\gamma/b) \tag{7}$$

where b is the Burgers vector.

To confirm the logic of the derivation of Eq. (2), and to determine the validity of the assumptions in deriving Eqs. (3) and (4), the equations for the mean and standard deviation of the source lengths were validated using a numerical simulation. Random locations for the source pins were generated using a fortran code and analyzed for statistical variations using a simple computer algorithm. Briefly, the algorithm evaluated the statistics of placing a fixed number of pins randomly on an oblique cylinder section using a random number generator. For a given total number of pins, say n, the longest of the shortest distances from the n points to the elliptical perimeter were calculated. This was repeated for different values of n. Using a thousand trials for each value of n, the mean and standard deviation of the longest segment was calculated. The results of the numerical algorithm are shown compared with the analytical model in Figure 2 for the case of slip plane orientation $\beta = 45°$. The analytical model is found to correspond very well with the numerical results, validating the model assumptions with respect to the Gaussian nature of the stochastics.

Experimental data are available for the effect of specimen size on the critical resolved shear stress of cylindrical microcrystals of nickel and gold [1–4]. The specimens range in size from 0.1 to 40 μm in diameter. The work on nickel microcrystals also report measured dislocation densities to be near $2\times 10^{12}/\text{m}^2$ [2]. In most cases the cylinder height was 2–3 times the sample diameter and the primary slip plane was nearly 45° to the loading axis. These experimental data are shown plotted along with model predictions in Figure 3. The predicted mean in Figure 3 was based on $\bar{\lambda}_{\max}$, while the upper and lower bounds shown were based on $(\bar{\lambda}_{\max} - \sigma_{\lambda_{\max}})$ and $(\bar{\lambda}_{\max} + \sigma_{\lambda_{\max}})$ respectively. The parameters used in the model for the two cases are given below.

From experiments: $\rho_{\text{tot}} = 2\times 10^{12}/\text{m}^2$; $s = 12$; $h = 2.5(2R)$; $\tau_0 = 11$(Ni), 13 (Au) MPa; $\beta = 45°$. Material parameters: nickel: $G = 76$ GPa, $b = 0.24$ nm, $\gamma = 0.2$ J/m^2; gold: $G = 27$ GPa, $b = 0.288$ nm, $\gamma = 0.05$ J/m^2.

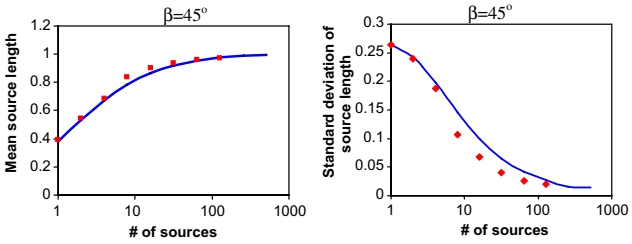

Figure 2. Results for the mean and standard deviation obtained from numerical simulations are shown compared with the analytical equations for the case of $\beta = 45°$. The calculations are for a cylinder with radius unity.

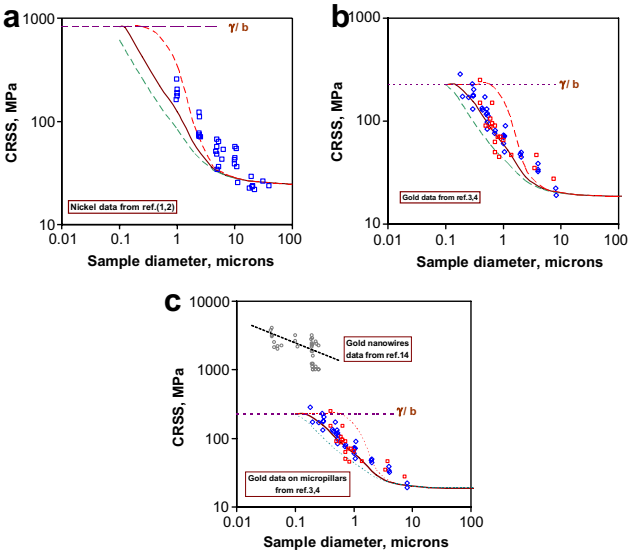

Figure 3. The model predictions for (a) nickel and (b) gold are shown in comparison with reported experimental data (from Refs. [1–4]). The dotted lines (green and red in the web version) correspond to the lower and upper standard deviations from the mean as predicted by the model. The plot in (c) includes data for gold nanowires (from Ref. [18]) to show that these differ from gold micropillars, suggesting that the nanowires are likely dislocation free with smooth surfaces that do not favor easy nucleation as in whiskers [8]. (For interpretation of the references in colour in this figure caption, the reader is referred to the web version of this article.)

Note that the values for dislocation density (ρ_{tot}), crystal orientation (β) and specimen height (h) are the same as the reported experimental values, while the remaining parameters are well-known material parameters. The friction stress, τ_0, is derived from the experimental bulk limit of the reported data by subtracting the contribution from the dislocation forest as given by Eq. (5). The only fit parameter was α, and this was taken to be unity. The effect of specimen size on the scatter is predicted using the second moment of the effective source length, as given by Eq. (4).

It can be seen from Figure 3 that a model that considers the statistical variation in the source length of dislocations imposed by finite dimensions of a cylindrical sample is sufficient to rationalize much of the effect of sample size on the measured flow stress of microcrystals. The predicted scatter for small samples is found to be reasonable, while the predicted scatter for larger samples is less than that observed. The latter could arise from variations in the initial dislocation density in real crystals. While this is satisfactory, the validity of the key assumptions of this model remains to be examined.

First, note that the model predicts only the initial stress for plasticity, i.e. CRSS, defined as strain resulting from the operation of a minimum of one source in the presence of a dislocation forest. Thus this stress includes a back stress that accounts for the forest hardening (assuming a size-independent Taylor relation); however, it neglects hardening from the mobile source interacting directly with the forest or secondary sources forming debris and junctions. The experimental data typically represent flow stress after 0.2% plastic strain. For a specimen of diameter 1 μm (height 2.5 μm), the passage of one dislocation through an entire slip plane amounts to a plastic shear strain of 10^{-4} ($=b/h$), or 0.01% per cycle of the source operation. For a strain of 0.2% the source will have to operate 20 times. This is not unreasonable, but in real crystals, strain hardening from direct interactions could occur, raising the external stress. Thus, predictions lower than experimental values indicate the degree of additional strain hardening in the real crystals.

Second, it is necessary to verify if the experimentally imposed strain rates are obtainable. The critical size of the sample is 1 μm, where the number of sources reaches the order of unity. For an imposed strain rate of $10^{-3}\,s^{-1}$ (typical in experiments) the source will have to operate 10 times per second. This amounts to an average velocity of the tip of the dislocation arm to be about 60 μm/s, which is reasonable. It is worth noting that, in larger samples, variations in the strain avalanches are seen in experiments [17]. These likely arise from the variations in how many sources operate at any given time, in addition to how they interact with the forest.

Third, the model assumes that the stress required to nucleate from the surface is not strength-limiting; rather, the glide resistance of a partial dislocation determines the upper bound. To determine the validity of this assumption, data on ultra-high-strength nanowires of gold were considered. Figure 3c shows that the data on gold micropillars differs from those obtained during bending of gold nanowires by Wu et al. [18]. It is suggested that this arises from the fact that nanowire flow stresses are limited by nucleation of dislocations from surfaces free of gross imperfections being related to the method of preparation, as has been suggested by Nadgorny for whiskers [8]. This provides indirect evidence that the micropillars are not limited by nucleation of dislocations.

Finally, it must be pointed out that in samples with only one source, the Schmidt factor might be lower and will produce a higher yield stress for a given critical resolved shear stress. For comparison with the model, the experimental data were reduced using the Schmidt factor of the primary slip system, due to lack of knowledge of the actual slip system.

In summary, it is shown that a model which considers the statistical variation in the source length of dislocations imposed by finite dimensions of a cylindrical sample is sufficient to rationalize much of the effect of sample size on the measured flow stress of microcrystals. Consideration of the key assumptions in comparison with typical experimental conditions has shown that the assumptions are reasonable. Comparison with data on nanowires shows that the measured flow stresses of micropillars are not nucleation controlled. It is suggested that strain avalanches observed in micropillars are due to the stochastics of the source operation.

This work was funded in part by US Air Force Contract No. FA8650-04-D-5233.

[1] M.D. Uchic, D.M. Dimiduk, J. Florando, W.D. Nix, Science 305 (2004) 986.
[2] D.M. Dimiduk, M.D. Uchic, T.A. Parthasarathy, Acta Mater. 53 (2005) 4065–4077.
[3] J.R. Greer, W.C. Oliver, W.D. Nix, Acta Mater. 53 (2005) 1821–1830.
[4] C.A. Volkert, E.T. Lilleodeen, Size effects in the deformation of sub-micron Au columns, Philos. Magn. 86 (2006) 5567–5579.
[5] N.A. Fleck, G.M. Muller, M.F. Ashby, J.W. Hutchinson, Acta Metall. Mater. 42 (1994) 475.
[6] K.W. McEhlaney, J.J. Vlassak, W.D. Nix, J. Mater. Res. 13 (1998) 1300.
[7] S.S. Brenner, J. Appl. Phys. 28 (1957) 023.
[8] E.M. Nadgorny, Soviet Phys. 5 (3) (1962) 462–476.
[9] J.C. Fischer, J.H. Holloman, AIME (1947) 2218.
[10] J.G. Sevillano, I.O. Arizcorreta, L.P. Kubin, Mater. Sci. Eng. 309–310 (2001) 393–405.
[11] V.S. Deshpande, A. Needleman, E.V.d. Giessen, J. Mech. Phys. Solids 53 (2005) 2661–2691.
[12] D.S. Balint, V.S. Deshpande, A. Needleman, E.V.d. Giessen, Model. Simul. Mater. Sci. Eng. 14 (2006) 409–422.
[13] A.A. Benzerga, N.F. Shaver, Scripta Mater. 54 (2006) 1937–1941.
[14] J.P. Hirth, H. Lothe, Theory of Dislocations, McGraw Hill Inc., 1968, p. 130.
[15] S.I. Rao, T.A. Parthasrathy, M. Tang, D.M. Dimiduk, M.D. Uchic, C. Woodward, Large-scale three-dimensional dislocation simulations reveal key mechanisms for strengthening at the micrometer scale, Nature, (in review).
[16] K. Gall, J. Diao, M.L. Dunn, Nano Lett. 4 (12) (2004) 2431–2436.
[17] D.M. Dimiduk, C. Woodward, R. LeSar, M.D. Uchic, Science 312 (2006) 1188–1190.
[18] B. Wu, A. Heidelberg, J.J. Boland, Nature Mater. 4 (2005) 525–529.